

Constraining planet formation around $6M_{\odot}$ - $8M_{\odot}$ stars

Dimitri Veras^{1,2*}†, Pier-Emmanuel Tremblay¹, J.J. Hermes³,
 Catriona H. McDonald^{1,2}, Grant M. Kennedy^{1,2‡}, Farzana Meru^{1,2§},
 Boris T. Gänsicke^{1,2}

¹Centre for Exoplanets and Habitability, University of Warwick, Coventry CV4 7AL, UK

²Department of Physics, University of Warwick, Coventry CV4 7AL, UK

³Department of Astronomy, Boston University, 725 Commonwealth Ave., Boston, MA 02215, USA

27 January 2020

ABSTRACT

Identifying planets around O-type and B-type stars is inherently difficult; the most massive known planet host has a mass of only about $3M_{\odot}$. However, planetary systems which survive the transformation of their host stars into white dwarfs can be detected via photospheric trace metals, circumstellar dusty and gaseous discs, and transits of planetary debris crossing our line-of-sight. These signatures offer the potential to explore the efficiency of planet formation for host stars with masses up to the core-collapse boundary at $\approx 8M_{\odot}$, a mass regime rarely investigated in planet formation theory. Here, we establish limits on where both major and minor planets must reside around $\approx 6M_{\odot} - 8M_{\odot}$ stars in order to survive into the white dwarf phase. For this mass range, we find that intact terrestrial or giant planets need to leave the main sequence beyond approximate minimum star-planet separations of respectively about 3 and 6 au. In these systems, rubble pile minor planets of radii 10, 1.0, and 0.1 km would have been shorn apart by giant branch radiative YORP spin-up if they formed and remained within, respectively, tens, hundreds and thousands of au. These boundary values would help distinguish the nature of the progenitor of metal-pollution in white dwarf atmospheres. We find that planet formation around the highest mass white dwarf progenitors may be feasible, and hence encourage both dedicated planet formation investigations for these systems and spectroscopic analyses of the highest mass white dwarfs.

Key words: planets and satellites: formation – protoplanetary discs – planets and satellites: dynamical evolution and stability – planet-star interactions – stars: white dwarfs – stars: AGB and post-AGB

1 INTRODUCTION

From the first detection of exoplanetary material one century ago (van Maanen 1917, 1919; but recognized as such only much later) to the pioneering discoveries of exoplanets over the last three decades (Campbell et al. 1988; Latham et al. 1989; Wolszczan & Frail 1992; Hatzes & Cochran 1993; Wolszczan 1994; Mayor & Queloz 1995; Marcy & Butler 1996), we are starting to piece together an understanding of planetary formation, evolution and fate. Major and minor planets, including asteroids, comets and planetary debris, have now been observed

orbiting brown dwarfs, M-type to B-type main-sequence stars, subgiant and red giant branch stars, white dwarfs, and pulsars. However, we still lack definitive detections in systems with O-type stars, asymptotic giant branch stars, and black holes¹.

On 21 Nov 2019, the NASA Exoplanet Archive listed as “confirmed” 4,099 major planets which have been discovered orbiting main-sequence, subgiant and giant branch stars. From that population, the most massive known planet host with a well-constrained (within 10 per cent) mass above $3.0M_{\odot}$ is o UMa b, whose host star mass is $3.09 \pm 0.07M_{\odot}$ (Sato et al. 2012). This detection cutoff at about $3.0M_{\odot}$ is not sharp, but rather represents a tail reflecting a decreasing

* E-mail: d.veras@warwick.ac.uk

† STFC Ernest Rutherford Fellow

‡ Royal Society University Research Fellow

§ Royal Society Dorothy Hodgkin Fellow

¹ Kervella et al. (2016) reported a so far unconfirmed candidate planet orbiting an asymptotic giant branch star.

number of discoveries as a function of stellar mass (see Fig. 5 of Reffert et al. 2015, Fig. 9 of Ghezzi et al. 2018 and Fig. 3 of Grunblatt et al. 2019).

This upper bound results from some combination of observational limitations and restrictions on where and how planets can form and evolve around stars more massive than the Sun (Kennedy & Kenyon 2008), and does not change depending on stellar classification (Lloyd 2011) nor whether asteroseismological constraints are taken into account (Campante et al. 2017; North et al. 2017; Stello et al. 2017).

The formation of planets around (low-mass) $\leq 3M_{\odot}$ stars represents one of the most extensively studied aspects of exoplanetary science. The two oldest formation theories are gravitational instability (Kuiper 1951; Cameron 1978; Boss 1997) (see Durisen et al. 2007, Helled et al. 2014, Kratter & Lodato 2016 and Rice 2016 for reviews), and core accretion (Safronov & Zvjagina 1969; Goldreich & Ward 1973; Perri & Cameron 1974; Harris 1978; Mizuno 1980) (see Pollack 1984 and Lissauer & Stevenson 2007 for reviews). More recently, important physical processes such as the streaming instability (Youdin & Goodman 2005; Johansen et al. 2007) and pebble accretion (Lambrechts & Johansen 2012) have provided alternatives or enhancements to the traditional formulations. Each theory, when combined with post-formation dynamical evolutionary pathways, succeeds in reproducing observed properties of some but not all of the known exoplanets.

All these formation processes require the presence of a circumstellar, protoplanetary disc, and operate in different regions of the disc on different timescales. A disc must survive long enough and be massive enough for a planet to form.

Unfortunately, like observations of main-sequence exoplanet host stars themselves, observations of protoplanetary discs are restricted by the rarity of massive host stars and the short lifetimes of their discs. Early on in the life of a stellar birth cluster, circumstellar discs have been observed to contain a wide variety of masses, up to host masses of many tens of solar masses (Forgan et al. 2016; Ilee et al. 2018; Jankovic et al. 2019; Sanna et al. 2019). Young, intermediate stars such as Herbig Ae/Be stars are commonly seen to host circumstellar discs, which are almost certainly sites of planet formation (much as T Tauri stars are precursors to planet-hosts like the Sun). Several of these stars have masses greater than $3M_{\odot}$ (Hernández et al. 2005), suggesting that a fertile circumstellar environment could exist for high host-star mass planet formation.

Here, we present another source of motivation to study planet formation around high-mass ($6M_{\odot} - 8M_{\odot}$) stars: the end state of these systems. As outlined in Section 2, current observations of white dwarfs with exoplanetary material expand the traditional main-sequence host-star mass range, and future observations could expand this range even further. In fact, the vast majority of $\gtrsim 3M_{\odot}$ stars ever formed and which now reside within a local volume of hundreds of parsecs are cooling white dwarfs.

Based on these prospects, we compute survival limits for the bounding case of the highest main-sequence host star

masses which would not trigger a core-collapse supernova² ($\approx 6M_{\odot} - 8M_{\odot}$) but instead become white dwarfs (which could eventually harbour observed metal pollution). In Sections 3 and 4 respectively we compute survival limits for both major and minor planets around these massive progenitors. We discuss our results in Section 5 and conclude in Section 6, hoping to motivate future dedicated investigations of planet formation around high-mass stars.

2 WHITE DWARF PLANET HOSTS

After both major and minor planets are formed and dynamically settle, the remainder of main-sequence evolution is thought to remain relatively quiescent. For example, in our solar system, over the last 4 Gyr or so, the orbits of the eight major planets have not varied enough to incite mutual scattering events. This quiet situation is very likely to continue until the end of the Sun’s main-sequence lifetime about 6 Gyr from now (Laskar & Gastineau 2009).

Subsequently, when the Sun ascends the giant branch phases, major changes (described in detail in Sections 3 and 4) will ensue. The surrounding bodies which survive these changes will eventually orbit a white dwarf, a stellar ember that is dense enough to stratify any accreted material into its constituent chemical elements (Schatzman 1945, 1947). This property enables the detection of exoplanetary metals, because predominantly white dwarf atmospheres would otherwise be composed of only hydrogen and/or helium.

2.1 Origin of exoplanetary material

These metallic debris seen in the atmospheres of single white dwarfs do not necessarily arise from major planets. In fact, signatures of individual minor planets have now been found around three different white dwarfs: WD 1145+017 (Vanderburg et al. 2015), SDSS J1228+1040 (Manser et al. 2019) and ZTF J0139+5245 (Vanderbosch et al. 2019).

These discoveries have corroborated observations of metal-polluted white dwarf photospheres. On both chemical and dynamical grounds, most of the atmospheric debris likely originates from exo-asteroids (Gänsicke et al. 2012; Jura & Young 2014; Veras 2016a; Harrison et al. 2018; Hollands et al. 2018; Doyle et al. 2019; Swan et al. 2019), exo-moons (Payne et al. 2016, 2017) or their fragments from destructive giant branch radiation (Veras et al. 2014a; Veras & Scheeres 2020). Minor planets, or their fragments, can avoid being engulfed into the star during the giant branch phases only at distances beyond several or many au (Mustill & Villaver 2012; Madappatt et al. 2016; Gallet et al. 2017; Rao et al. 2018; Sun et al. 2018). Therefore, at least one (surviving) major planet must exist in these

² Wada et al. (2019) considered planet formation around super-massive black holes which are just a few parsecs away from active galactic nuclei. However, the prospects of detecting planetary systems outside of the Milky Way Galaxy are currently remote, except perhaps for the Large Magellanic Cloud (which probably does not contain a central black hole; Covone et al. 2000; Ingresso et al. 2009; Lund et al. 2015; Mróz, & Poleski 2018).

systems to perturb the minor bodies into the disruption region around the white dwarf from au-scale distances, as argued extensively in Veras et al. (2018a).

What if the white dwarf is currently observed to have a binary stellar companion (Pyrzas et al. 2012; Wilson et al. 2019)? Then, debris in the white dwarf atmosphere could originate from the winds of its partner rather than a planetary system. However, if the companion is separated beyond a critical distance, then the accreted mass from the wind would be too small to explain the observations (and hence must arise from a planetary system). This critical distance is on the order of few au (Debes 2006; Veras et al. 2018a), well within the binary separation for the majority of known polluted white dwarfs in binaries.

What if, instead, a polluted white dwarf *used to* have a binary stellar companion which underwent a merger³? Could the atmospheric debris then result from the merger event? The answer is no, because any metal mixing resulting from the merger would sink to the core very quickly, on a timescale which is 3-11 orders of magnitude shorter than the cooling age (Koester 2009; Dufour et al. 2010; Bauer & Bildsten 2018, 2019; Cunningham et al. 2019). Hence, no chemical signatures from the merger would be currently observable.

In summary, regardless if a white dwarf has or had binary companions, *both major and minor planets should exist in metal-polluted systems without stellar binary companions and whose main-sequence progenitor masses were 6 M_{\odot} – 8 M_{\odot}* . So far major planets in such high mass systems have not been observed⁴. However, the statistics of high-mass metal rich white dwarfs are still poorly understood, owing to the steepness of the initial mass function and their faintness, and therefore their rarity (Tremblay et al. 2016).

2.2 The most massive white dwarf host

Unlike for main-sequence exoplanetary systems, white dwarf planetary systems are not yet summarized with a publicly-available database. Rather, this data is contained within different published studies (Dufour et al. 2007; Kleinman et al. 2013; Gentile Fusillo et al. 2015; Kepler et al. 2015, 2016; Hollands et al. 2017; Gentile Fusillo et al. 2019; Coutu et al. 2019).

Nevertheless, we can identify the most massive polluted white dwarf host based from individual observing campaigns. The homogeneous sample of bright, hydrogen-atmosphere white dwarfs studied in Koester et al. (2014) reveals that the metal polluted WD 1038+633 has a robust mass determination both from Balmer line spectroscopy

³ Cheng et al. (2019) have recently suggested that 20 ± 6 per cent of high-mass white dwarfs ($1.08M_{\odot}$ – $1.23M_{\odot}$) originate from double white dwarf mergers (Toonen et al. 2012; Shen et al. 2012; García-Berro et al. 2012). In addition, another significant fraction are likely merger byproducts merged when at least one of the stellar components was not a white dwarf (Toonen et al. 2017; Temmink et al. 2019).

⁴ However, see Gänsicke et al. (2019) for robust evidence of a major ice giant planet orbiting a white dwarf whose progenitor mass was $1.0M_{\odot}$ – $1.6M_{\odot}$; Veras & Fuller (2020) has suggested that this giant planet is a partially destroyed and highly inflated “Super-Puff”.

($M_{\text{WD}} = 0.90 \pm 0.01 M_{\odot}$; Tremblay et al. 2011) and from *Gaia* photometry and astrometry ($M_{\text{WD}} = 0.91 \pm 0.01 M_{\odot}$; Gentile Fusillo et al. 2019). The progenitor mass is more uncertain, but Koester et al. (2014) estimate a value of $\approx 4 M_{\odot}$.

In a different investigation, Coutu et al. (2019) analysed a sample of helium-atmosphere white dwarfs with metal pollution mostly drawn from the Sloan Digital Sky Survey (SDSS). Their figure 10 demonstrates that for a generous upper limit of 10% precision on *Gaia* parallax, the most massive currently known progenitor of a metal polluted white dwarf is similarly $\approx 4 M_{\odot}$, albeit with larger error bars on the white dwarf mass.

In either case, the most massive currently observed metal-polluted white dwarf contains a progenitor mass of about $4M_{\odot}$. In Section 5, we will elaborate on the exciting and imminent increase in the number of polluted white dwarfs for which spectroscopy will be obtained, and the prospects for finding even higher mass hosts.

2.3 Main-sequence progenitor masses

Extrapolating measured white dwarf masses to main-sequence values requires the application of an initial-to-final-mass relation. This relation, however, is poorly constrained in the $6M_{\odot}$ – $8M_{\odot}$ regime. Observationally, Figure 5 of Cummings et al. (2018) reveals that white dwarf masses higher than about $1.05M_{\odot}$ plausibly correspond to main-sequence masses of about $6M_{\odot}$ – $8M_{\odot}$, with large uncertainties; the lower mass boundary for a core-collapse supernova to occur is $8M_{\odot} \pm 1M_{\odot}$ (Smartt 2009).

Plots for the maximum envelope radius, phase durations, main sequence age, and mass loss for 6 – $8M_{\odot}$ stars based on the SSE stellar evolution code (Hurley et al. 2000) have already all been presented in Veras et al. (2013a) and we do not repeat them here. Instead, we reiterate the most important of those features in Table 1. Variations in these numbers which would arise from the application of other stellar codes are small enough to not qualitatively affect our results, especially given the uncertainty in the initial-to-final-mass relation.

2.4 Short main-sequence lifetimes

One set of values from Table 1 which deserves special attention is the duration of the main sequence phase (35-70 Myr). Hence, subsequent to protoplanetary disc dissipation, for $6M_{\odot}$ – $8M_{\odot}$ systems, only a few to several tens of Myr would remain before the host star leaves the main sequence. This period of time might have been too short for the giant planets in our own solar system to dynamically settle (e.g. Tsiganis et al. 2005; Morbidelli et al. 2018). Nevertheless, significant gravitational scattering events may occur earlier in other systems, before the end of the main sequence phase.

Even during the main-sequence phase of these systems, planets are subject to other forces which are often neglected in other exoplanetary studies. In the most extreme case of a $8M_{\odot}$ host star, the star will actually lose 3.4 per cent of its mass by the end of the main sequence. In contrast, the Sun will lose no more than 0.06 per cent of its mass

Table 1. Some stellar evolution properties for given zero-age-main-sequence (ZAMS) mass and metal mass fraction (given through the quantity Z) tracks based on the SSE code. “AGB” is an abbreviation for asymptotic giant branch. For the metal-poor $Z = 0.0001$ case, the $7M_{\odot}$ and $8M_{\odot}$ stars become neutron stars, and hence we do not consider them further.

ZAMS mass (M_{\odot})	Z	white dwarf mass (M_{\odot})	main sequence duration (Myr)	AGB duration (Myr)	Max R (au)	Max L (L_{\odot})	Max T (K)
6.00	0.02	1.14	66.0	0.56	5.94	6.16×10^4	4.12×10^5
6.00	0.0001	1.37	60.0	0.75	4.29	1.54×10^5	6.93×10^5
7.00	0.02	1.29	48.9	0.51	6.73	7.67×10^4	5.07×10^5
8.00	0.02	1.44	37.2	0.49	7.39	9.16×10^4	1.11×10^6

before the end of the main sequence (Veras & Wyatt 2012; Airapetian & Usmanov 2016). Further, how planet formation within protoplanetary discs is affected by such a rapidly changing massive star remains uncertain.

2.5 White dwarf disc lifetimes

Another important aspect of white dwarf planetary system observations is their age, because that parameter helps constrain dynamical history. The “cooling age” in particular refers to the time since the white dwarf was born. Metal polluted white dwarfs with cooling ages longer than about 100 Myr have metal sinking timescales in the atmosphere that range from just a few weeks to a few Myr (Koester 2009)⁵.

Such a short sinking timescale relative to the cooling age implies that metal pollution arises from a steady accretion stream originating in a ring- or disc-like planetary debris structure; these structures have now been observed in over 40 systems (e.g. Zuckerman & Becklin 1987; Graham et al. 1990; Gänsicke et al. 2006; Farihi 2016; Dennihy et al. 2018) and many others are likely hidden from view (Bonsor et al. 2017). Supporting the accretion stream theory is that white dwarfs, being Earth-sized, represent targets which are too small for direct hits by minor planets scattered from distances of many au (Brown et al. 2017).

The lifetime of those discs provides a hint as to when the surviving major planet (or planets) perturbed a minor planet (or its fragments) towards the white dwarf. Without considering any disc replenishment mechanisms (Grishin & Veras 2019; Makarov & Veras 2019), the lifetime of these discs is estimated to be $\sim 10^4 - 10^6$ yr (Girven et al. 2012). Because these timescales are still much smaller than a typical cooling age of at least 100 Myr, in this case the major planet did not trigger the pollution of the star immediately after it became a white dwarf, and the planet must have survived for at least 100 Myr of white dwarf cooling.

3 MAJOR PLANET SURVIVAL

Theoretical efforts to link main-sequence and white dwarf planetary systems in the highest-mass regimes have been

sparse. Veras et al. (2011, 2013a) and Voyatzis et al. (2013) did previously consider the evolution of major planets around $6M_{\odot} - 8M_{\odot}$ host stars. Since 2013, however, the focus has shifted towards much lower stellar masses (typically $3M_{\odot}$ and below) because those were the only ones which matched the mounting number of observations over this period (see in particular the match between the results of Mustill et al. 2018 and Hollands et al. 2017, 2018). In this section, we provide a significantly updated assessment of the basic survival considerations from Veras et al. (2013a) and Voyatzis et al. (2013).

As argued earlier, in order for the eventual white dwarf to be polluted at a cooling age of hundreds of Myr, at least one major planet needs to survive until the white dwarf phase, and then for at least another approximately 100 Myr. Subsequently the major planet would kick a minor planet or debris towards the white dwarf (with the travel time being less than 1 Myr). A disc is then formed, and that disc would accrete onto the star on a timescale less than about 1 Myr.

Now we detail how the major planet can survive until the white dwarf phase.

3.1 Orbital expansion due to mass loss

During the giant branch phases, orbits will expand due to stellar mass loss (Omarov 1962; Hadjidemetriou 1963; see Section 4 of Veras 2016a for a historical summary). For isotropic mass loss, an “adiabatic” regime may be defined where the orbital eccentricity remains nearly constant as the semimajor axis is increased (Veras et al. 2011). In this regime, the semimajor axis increases inversely to the mass which remains, such that, for example, a 75 per cent mass loss quadruples the semimajor axis. The boundary of the adiabatic regime scales with stellar mass. However, Figs. 14–15 of Veras et al. (2011) illustrate that despite the high mass loss rate from $6 - 8M_{\odot}$ stars, the resulting change in eccentricity for orbiting bodies within 100 au remains negligible (and in the adiabatic regime).

If the mass loss is instead anisotropic, then the character of the orbital expansion changes (Veras et al. 2013b; Dosopoulou & Kalogera 2016a,b). However, the potential anisotropy of the mass loss from $6 - 8M_{\odot}$ stars is not well-constrained, and evidence from planetary nebulae remain in the realm of binary stars (e.g. Hillwig et al. 2016). Only significant sustained anisotropy would change the orbital evolution of a planet within 100 au from its predicted isotropic adiabatic value (Veras et al. 2013b).

⁵ The lower end of the range corresponds to warm hydrogen-atmosphere (DA class) white dwarfs.

In summary, given the mass values in Table 1, the semi-major axis of an orbiting planet would likely increase by a factor of 4.4–5.6. For the lower mass stars usually considered in post-main-sequence planetary science studies, this factor is instead about 2–4 (Fig. 3 of Veras 2016a).

3.2 Orbital engulfment due to tidal interactions

As the star is losing mass and the planet’s orbit is expanding, the star is expanding as well. In fact, the stellar envelope may expand quickly enough and close enough to the planet to draw it inside. Many investigations have computed the critical engulfment distance (technically the minimum star-planet separation on the main sequence which leads to engulfment on the giant branches) for the red giant branch phase (Villaver & Livio 2009; Kunitomo et al. 2011; Villaver et al. 2014; Gallet et al. 2017; Rao et al. 2018; Sun et al. 2018), the asymptotic giant branch phase (Mustill & Villaver 2012), or both phases (Adams & Bloch 2013; Nordhaus & Spiegel 2013; Madappatt et al. 2016).

The approaches and prescriptions in the papers listed above differ. Here we seek just a rough estimate. Further, for 6–8 M_{\odot} stars, the red giant branch phase is negligibly short. Consequently, the extremes of luminosity, temperature and radius all occur close to, but not precisely at, the tip of the asymptotic giant branch phase.

Hence, we focus on this latter phase only. Mustill & Villaver (2012) carried out detailed numerical simulations which determined the critical engulfment distance of different types of planets (different masses and compositions) around asymptotic giant branch stars whose main-sequence progenitor masses went up to 5 M_{\odot} . They used the equilibrium tidal model of Zahn (1977) for their formalism. Adams & Bloch (2013) instead took a different approach, and derived an analytical formula for the critical engulfment distance, d_{eng} , as a function of several free parameters. Their prescription includes a correction for pulsations during the asymptotic giant branch phase. Neither study adopted stellar metallicity as a free parameter⁶.

Let us assume the extreme quiescent case of a planet forming on a circular orbit around stars more massive than 5 M_{\odot} . Extrapolating Fig. 7 of Mustill & Villaver (2012) yields the following crude estimates for Jovian, Neptunian and terrestrial planets:

$$d_{\text{eng}}^{(\text{Jovian})} = 0.48 \text{ au} \left(\frac{M_{\star}}{M_{\odot}} \right) + 2.6 \text{ au} \quad (1)$$

$$= \{5.5, 6.0, 6.4\} \text{ au},$$

$$d_{\text{eng}}^{(\text{Neptunian})} = 0.33 \text{ au} \left(\frac{M_{\star}}{M_{\odot}} \right) + 1.8 \text{ au} \quad (2)$$

$$= \{3.8, 4.1, 4.4\} \text{ au},$$

$$d_{\text{eng}}^{(\text{Terrestrial})} = 0.28 \text{ au} \left(\frac{M_{\star}}{M_{\odot}} \right) + 1.42 \text{ au} \quad (3)$$

$$= \{3.1, 3.4, 3.6\} \text{ au},$$

⁶ More massive progenitor stars should have higher metallicities because they must be younger if they are evolved from single stars.

where the evaluations above correspond to ZAMS masses of $M_{\star} = \{6, 7, 8\} M_{\odot}$.

Equations 32 and 38 of Adams & Bloch (2013) instead give

$$\frac{d_{\text{eng}}}{2 \text{ au}} \approx \left[\mathcal{P} \left(\frac{q+1}{q+\beta-p-1} \right) \left(\frac{\tau}{0.1 \text{ Myr}} \right) \left(\frac{M_{\text{planet}}}{M_{\text{Jupiter}}} \right) \right]^{2/19} \times \left(\frac{M_{\star}}{M_{\odot}} \right)^{-1/19} \left(\frac{R_{\star}}{1 \text{ au}} \right)^{16/19}. \quad (4)$$

In equation (4), τ represents a mass loss timescale; here we use the duration of the asymptotic giant branch phase (see Table 1). The coefficient $\mathcal{P} > 1$ represents the enhancement factor due to the presence of pulsations. The indices q , p and β respectively represent the radial dissipation index, the mass loss index and the mass dissipation index. Although these values are free parameters, Adams & Bloch (2013) stated that the critical value of the tidal dissipation parameter, which is a component of equation (4), is accurate to within 50 per cent across the entire parameter space.

Our own numerical investigation reveals that the leading term with the indices varies by less than 20 per cent across all plausible values of q , p and β . Hence, we simply adopt $q = 7$, $\beta = 2$, and $p = 0$, such that the leading term is unity. We also take both M_{\star} and R_{\star} to represent the mass and radius of at the star at the start of the asymptotic giant branch phase. Then for ZAMS masses of $M_{\star} = \{6, 7, 8\} M_{\odot}$, we obtain

$$d_{\text{eng}}^{(\text{Jovian})} = \{4.0, 4.3, 4.5\} \mathcal{P} \text{ au}, \quad (5)$$

$$d_{\text{eng}}^{(\text{Neptunian})} = \{3.0, 3.2, 3.3\} \mathcal{P} \text{ au}, \quad (6)$$

$$d_{\text{eng}}^{(\text{Terrestrial})} = \{2.2, 2.4, 2.5\} \mathcal{P} \text{ au}. \quad (7)$$

Figure 4 of Adams & Bloch (2013) illustrates that the pulsation enhancement factor \mathcal{P} can change the engulfment boundary by several tens of per cent. Hence, the values of d_{eng} from the two different sets of assumptions and extrapolations employed here may be roughly consistent. We show the correspondence in Fig. 1.

3.3 In-spiral inside stellar envelope

A planet engulfed in a stellar envelope is not necessarily immediately destroyed. The possibility exists that the planet may survive the resulting in-spiral. If so, the envelope – which is initially puffed up by the planet ingestion (Staff et al. 2016) – would have to dissipate before the planet becomes compressed and flattened by ram pressure (Jia & Spruit 2018). Planets themselves are typically too small to unbind the envelope (Nordhaus & Blackman 2006), and so survival would depend on a slow in-spiral.

By using orbital decay power scalings, MacLeod et al. (2018) compute, in their Figure 4, the in-spiral timescale in terms of orbits for a Jovian planet across parts of the Hertzsprung-Russell diagram. In every case the number of in-spiral orbits is less than, and usually much less than, 10^4 orbits. At most then, the in-spiral time represents about 10 per cent of the duration of the asymptotic giant branch phase.

The in-spiral time is hence effectively negligible. This conclusion, however, is extrapolated from just the handful

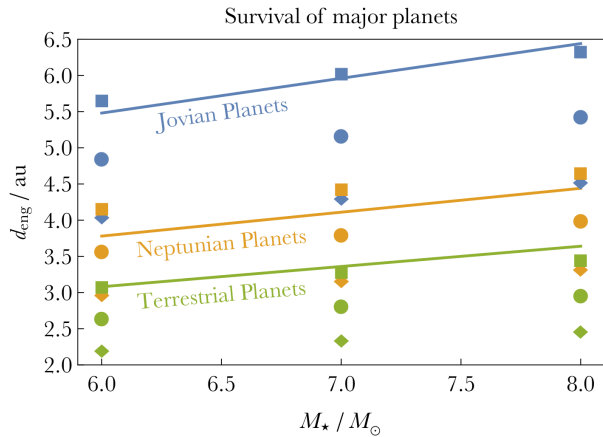


Figure 1. Minimum main-sequence star-planet distances (d_{eng}) for which a major planet will avoid engulfment in the asymptotic giant branch stellar envelope and survive until the white dwarf phase. The solid lines are simple linear extrapolations from Mustill & Villaver (2012) and the symbols are applications of Adams & Bloch (2013). The diamonds represent the (unrealistic) case when no pulsations along the asymptotic giant branch phase are taken into account. The circles and squares assume a pulsation enhancement factor of 20 and 40 per cent, respectively. The stars are assumed to have solar metallicity.

of papers above, which focus on the highest mass planets and stars with masses lower than those we consider here. More detailed modelling across a wider parameter space would provide a necessary complement to the tidal studies cited in Section 3.2.

Other related investigations have focused on the consequences for the parent star. Nelemans & Tauris (1998) illustrated that engulfment could lead to an under-massive white dwarf. Potential lithium enhancement due to planet engulfment (Carlberg et al. 2012, 2013; Stephan et al. 2019) would no longer be observable by the time the star becomes a white dwarf. However, rotational spin-up of the giant branch star due to engulfment (Massarotti 2008; Stephan et al. 2019) might leave a small but lasting residue, because the spin period of the eventual white dwarf would affect tidal interactions with orbiting planets (Veras et al. 2019a; Veras & Wolszczan 2019; Veras & Fuller 2019, 2020).

The residue perhaps also is manifest in the resulting change of magnetic field strength (Farihi et al. 2011; Kissin & Thompson 2015). The *Gaia*-SDSS spectroscopic white dwarf catalog in Gentile Fusillo et al. (2019) reveals that up to 50% of white dwarfs whose progenitors had masses of $6 - 8M_{\odot}$ have magnetic fields above the typical 1 MG detection limit (Kepler et al. 2013). This fraction could, however, represent a signature of the large fraction of massive white dwarfs that are thought to originate from mergers (García-Berro et al. 2012; Toonen et al. 2017; Cheng et al. 2019).

3.4 Gravitational scattering

Even if a planet survives tidal interactions with the star and, if applicable, in-spiral inside the envelope, the planet may then be subject to gravitational interactions with other, more distant surviving planets. The result could be ejection

from the system, collision with the star or collision with the other planet.

Gravitational scattering between multiple major planets in giant branch planetary systems has been investigated in only about one dozen papers (an order of magnitude smaller than the comparable body of literature for multi-planet scattering in main-sequence planetary systems). Nevertheless, we know that in evolving single-star exo-systems, stellar mass loss can trigger instability due to changes in the Hill stability limit (Debes & Sigurdsson 2002; Veras et al. 2013a; Voyatzis et al. 2013; Veras et al. 2018b), Lagrange stability limit (Mustill et al. 2014; Veras & Gänsicke 2015; Veras et al. 2016; Mustill et al. 2018) and shifting location of secular resonances (Smallwood et al. 2018, 2019a). Further, the combined effect of mass loss and Galactic tides can incite instability from a distant massive planetary companion (like the theorized “Planet Nine”; see Batygin et al. 2019 for a review) in an otherwise quiescent system (Veras 2016b).

The timescale over which the instability acts would be crucial for evolved $6 - 8M_{\odot}$ planetary systems. The only two of the above-cited papers which has simulated multi-planet instability in $6 - 8M_{\odot}$ systems are Veras et al. (2013a) and Voyatzis et al. (2013). Figures 9-12 of Veras et al. (2013a) reveal that instability time is unrestricted but strongly dependent on the initial separations of the planets. Further, instability is relatively rare during the giant branch phases, particularly for the shortest such phases at the highest stellar masses. This rarity suggests that gravitational instability is unlikely to feature until the star has become a white dwarf.

A plausible scenario is that gravitational instability amongst multiple planets (which survived the giant branch phases of evolution) occurred a few hundred Myr after the parent star became a white dwarf. These timescales match with instability timescales for plausible sets of initial conditions from the studies above (by extrapolating from lower stellar masses). Nevertheless, multiple planets are not actually required to pollute the white dwarf with minor planets (Bonsor et al. 2011; Debes et al. 2012; Frewen & Hansen 2014; Antoniadou & Veras 2016, 2019), but can facilitate the process (Veras et al. 2016; Mustill et al. 2018; Smallwood et al. 2018, 2019a).

4 MINOR PLANET SURVIVAL

The predominant focus in the exoplanet formation literature has been on major planets. However, white dwarf metal pollution highlights the need to also model minor planet formation. In fact, almost all observations of white dwarf planetary systems are of the remnants of minor planets.

By “minor planets”, we refer to an object with a mean radius of under 10^3 km. This size regime encompasses moons, comets, asteroids, and large fragments of major planets. In fact, the minor planet currently orbiting the white dwarf WD 1145+017 may best be classified as an “active asteroid” (Vanderburg et al. 2015) whereas the one orbiting SDSS J1228+1040 is perhaps best described as a ferrous chunk of a fragmented planetary core (Manser et al. 2019). The third, which orbits ZTF J0139+5245 (Vanderbosch et al. 2019), still defies classification, until at least more data is obtained.

These distinctions are becoming increasingly relevant given our detailed knowledge of white dwarf planetary systems. A related question of interest is whether white dwarf metal pollution arises from primarily intact or destroyed minor planets, and the locations at which those bodies or debris were scattered. The answer depends more strongly on radiation than gravity (Veras et al. 2015a) through the Yarkovsky and YORP effects.

The Yarkovsky and YORP effects are recoil forces and torques produced due to non-uniform scattering of absorbed radiation (Vokrouhlický et al. 2015). The Yarkovsky effect changes the orbit of a spherical or aspherical minor planet, whereas the YORP effects spins up or/and spins down an aspherical minor planet. Both effects have been modelled for solar system asteroids in exquisite detail (e.g. Rozitis & Green 2012, 2013; Cotto-Figueroa et al. 2015; Yu et al. 2018; Hirabayashi & Scheeres 2019). Contrastingly, only a handful of basic dedicated extrasolar post-main-sequence studies have been published for the Yarkovsky effect (Veras et al. 2015a, 2019b) and the YORP effect (Veras et al. 2014a; Veras & Scheeres 2020).

This contrast does not suit the added complexity introduced in giant branch systems, when the luminosity of the parent star changes on short timescales, and can be five orders of magnitude higher than the Sun’s (see Table 1). Such high luminosities easily fling exo-asteroids out to distances of tens, hundreds or even thousands of au, regardless of the presence of major planets, which only temporarily impede such migration (Veras et al. 2019b). These minor planets could also be propelled inwards, and the direction of motion is a function of the bulk shape, spin, surface topography and internal homogeneities of the objects.

If, however, the minor planets veer too close to a giant branch star, then they could be spun up to disruption. This rotational fission occurs when the spin of a minor planet reaches the critical spin failure rate ω_{fail} . For strengthless rubble piles in the solar system, this rate corresponds to a rotational period of about 2.3 hours and has robust confirmation through observations (Warner et al. 2009; Scheeres et al. 2015; Polishook et al. 2017).

Veras et al. (2014a) demonstrated that asteroid belts within about 7 au of their parent stars along the main sequence (including the solar system’s asteroid belt) would be easily fragmented by YORP-induced rotational fission along the giant branch phases. However, they considered parent stars with main sequence masses of 1 – 5 M_{\odot} .

Now we extend their study to higher stellar masses. The spin of a minor planet evolves according to Scheeres (2007, 2018)

$$\frac{d\omega(t)}{dt} = \frac{3\mathcal{C}\Phi}{4\pi\rho R^2 a(t)^2 \sqrt{1-e(t)^2}} \left(\frac{L_{\star}(t)}{L_{\odot}} \right) \quad (8)$$

where ρ and R represent the minor planet’s density and initial radius (both assumed to remain constant), and a and e represent its time-dependent semimajor axis and eccentricity. \mathcal{C} is a constant which represents the extent of the minor planet’s asphericity, and $\Phi = 1 \times 10^{17}$ kg·m/s² is the Solar radiation constant.

Equation (8) helps illustrate that the increasing luminosity of the star competes against the increasing semimajor axis from stellar mass loss. As previously mentioned, for adiabatic mass loss, the eccentricity remains constant. We

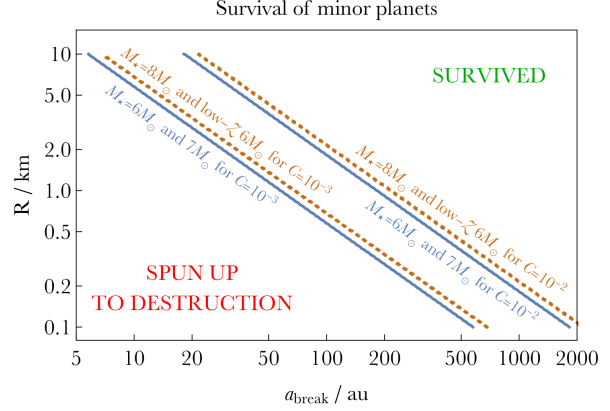


Figure 2. Minimum main-sequence semi-major axis (a_{break}) for which a minor planet will not spin up to breaking point by asymptotic giant branch radiation and survive until the white dwarf phase. The minor planet’s density is assumed to be 2 g/cm³ and we apply two values for its topological asphericity parameter ($\mathcal{C} = 10^{-2}, 10^{-3}$). The curves for the $Z = 0.02$, $M_{\star} = 6M_{\odot}$ and $Z = 0.02$, $M_{\star} = 7M_{\odot}$ cases are visually indistinguishable. Coincidentally, so are the curves for the $Z = 0.02$, $M_{\star} = 8M_{\odot}$ and $Z = 0.0001$, $M_{\star} = 6M_{\odot}$ cases. The minor planets are assumed to be strengthless rubble piles, initially have zero spin, and are assumed to never spin down throughout their evolution.

simply set it to zero here. An analytic expression of the failure rate which includes the minor planet’s tensile, uni-axial strength S is (Sánchez & Scheeres 2014; Scheeres 2018)

$$\omega_{\text{fail}} = \sqrt{\frac{4\pi G\rho}{3} + \frac{4S}{3\rho R^2}}. \quad (9)$$

We now compute simple estimates of a_{break} , the minimum initial (ZAMS) semimajor axis for which a minor planet will survive asymptotic giant branch YORP spin-up and reach the white dwarf phase. To do so, we integrate equation (8) assuming $S = 0$, $e = e(t) = 0$ and an initially non-spinning minor planet. We also assume that the asteroid does not spin down at any point during its evolution, and its asphericity is encompassed entirely within the assumed constant value of \mathcal{C} . We consider the YORP effect in isolation, decoupled from the Yarkovsky effect; such a coupling would require a significant modelling effort, and has not yet been achieved in exoplanetary science.

Figure 2 illustrates the result in $a_{\text{break}}-R$ space, across a range of R (100 m – 10 km) for which the YORP effect is significant. Coincidentally, the curves for the $Z = 0.02$, $6M_{\odot}$ and $7M_{\odot}$ cases are visually indistinguishable on the plot, as are the curves for the $Z = 0.02$, $8M_{\odot}$ and $Z = 0.0001$, $6M_{\odot}$ cases. Changing the asphericity parameter by one order of magnitude noticeably shifts the curves.

In comparison to the survival capacity of major planets, we find that across almost the entire phase space, $a_{\text{break}} > d_{\text{eng}}$ and usually, $a_{\text{break}} \gg d_{\text{eng}}$. However, in individual cases, these relations do not prevent the major planet from, for example, residing exterior to intact minor planets. Nevertheless, the relations suggest that a surviving major planet which is surrounded by fragmented debris is not an unreasonable scenario.

An important related question is whether a minor planet would be sublimated from the host star before or

during YORP spin-up. In order to estimate the sublimation rate of a minor planet, we use the approximation employed by Jura (2008); for a more detailed description of its physical assumptions, see Section 6.1.1. of Veras (2016a). The radius of a minor planet evolves according to

$$\frac{dR}{dt} = -\frac{1.5 \times 10^{10} \text{ kg} \cdot \text{m}^{-2} \text{ s}^{-1}}{\rho} \sqrt{\frac{T_{\text{sub}}}{T(t)}} \exp\left(-\frac{T_{\text{sub}}}{T(t)}\right) \quad (10)$$

where, with the the sublimation temperature T_{sub} and the Stefan-Boltzmann constant σ , the temperature of the minor planet T can be approximated by

$$T(t) = \left(\frac{L_{\star}(t)}{16\pi\sigma r(t)^2}\right)^{1/4}. \quad (11)$$

The functional form of equation (10) reveals a strong dependence on the ratio $T_{\text{sub}}/T(t)$, and the value of T_{sub} is composition-dependent. For olivine, $T_{\text{sub}} \approx 6.5 \times 10^4$ K. By adopting this value, along with $\rho = 2$ g/cm³, we find that the sublimation rate is negligible across almost the entire parameter space and can be ignored. For example, at the inner edge of this space, we find that for $r = \{20, 15, 10\}$ au, the *maximum* sublimation rate, as measured by radius decrease, across all of our $Z = 0.02$ stellar evolution tracks are, respectively, $\{2 \times 10^{-11}, 5 \times 10^{-8}, 6 \times 10^{-4}\}$ m/yr. Instead, for the $Z = 0.0001$, $M = 6M_{\odot}$ track, there is a greater danger at 10 au, with corresponding *maximum* sublimation values of $\{3 \times 10^{-8}, 3 \times 10^{-5}, 1 \times 10^{-1}\}$ m/yr.

Given that these minor planets largely survive sublimation, one may inquire about the size distribution of the debris which results from YORP-based break-up. Although this topic requires further dedicated study, Veras & Scheeres (2020) explored this size distribution in a basic, analytical fashion, based on the results of Scheeres (2018). Veras & Scheeres (2020) estimated the total number of fissioned components of an asteroid, as well as the sizes of the components, based on a number of factors including internal strength, initial spin and stellar luminosity. The result is hence dependent on many parameters and assumptions. The resulting dust produced may be blown away due to radiation pressure by comparing the interplay between radiation and gravity (Veras et al. 2015a); the presence of a major planet would affect this balance, and affects the regions where dust is ejected in a non-trivial fashion (Zotos & Veras, In Preparation).

5 DISCUSSION

Having computed the survival limits for both major and minor planets orbiting $6M_{\odot} - 8M_{\odot}$ stars, we now discuss topics which are related to these findings.

5.1 Ice line locations

Giant planets are commonly assumed to have formed beyond the ice line (or “snow line” or “frost line”)⁷, where volatile compounds condense. For $1M_{\odot}$ stars, the ice line is often assumed to reside at about 2.7 au (Hayashi 1981), exterior to d_{eng} .

⁷ See Batygin et al. (2016) for a challenge to the canonical theory.

However, as the host star mass increases, the relation between the ice line distance (denoted as d_{ice}) and d_{eng} does not become immediately clear. In the ZAMS stellar mass range considered in this paper, d_{eng} for giant planets is between about 5.5 and 6.5 au (Fig. 1).

In these same systems, the location of the ice line is determined by a combination of stellar irradiation and viscous heating. However, discs around massive stars are dispersed rapidly (Hernández et al. 2005), allowing the effect of irradiation to dominate. In this limit, we can approximate the midplane ice-line temperature T_{ice} just as Kennedy & Kenyon (2008) did by applying the following flared-disc prescription from Adams & Shu (1986), Kenyon & Hartmann (1987) and Chiang & Goldreich (1997):

$$T_{\text{ice}} = T_{\star} \left(\frac{\alpha}{2}\right)^{1/4} \left(\frac{R_{\star}}{d_{\text{ice}}}\right)^{3/4} \quad (12)$$

with

$$\alpha = 0.005 \left(\frac{d_{\text{ice}}}{1 \text{ au}}\right)^{-1} + 0.05 \left(\frac{d_{\text{ice}}}{1 \text{ au}}\right)^{2/7}. \quad (13)$$

By setting $T_{\text{ice}} = 170$ K and ZAMS values for R_{\star} and T_{\star} from the aforementioned `sse` code, we find that $d_{\text{ice}} = 2.4 - 3.6$ au $\approx 0.5d_{\text{eng}}$. Hence, even in this rough approximation, the engulfment distance along the giant branch phases is more restrictive than the ice line with regard to giant planet formation location.

The theoretical considerations in this subsection help motivate dedicated planet formation studies for high host-star mass systems. We now present observational motivation.

5.2 Future white dwarf host mass increases

Gaia is expected to discover, through astrometry, at least a dozen giant planets orbiting white dwarfs at the final data release (Perryman et al. 2014). If realized, this exciting prediction would revolutionize our understanding of white dwarf planetary systems⁸, but is highly unlikely to increase the mass of the most massive known white dwarf host star.

Instead, the new “record-breaker” is more likely to arise from the steep and imminent increase in known polluted white dwarfs. This increase will arise from the larger number of new white dwarfs which have already been identified from *Gaia*. *Gaia* Data Release 2 (Gaia Collaboration et al. 2018) recently uncovered an all-sky sample of $\approx 260,000$ white dwarf candidates that is homogeneous down to $G < 20$ mag (Gentile Fusillo et al. 2019). From this sample, on the order of 10,000 white

⁸ Some current observational limits have been placed on the possible locations of major planets orbiting white dwarfs. Null results in a deep *Spitzer* survey can rule out at least >10 Jupiter-mass planets within the 5-50 au range around more than 40 white dwarfs (Farihi, Becklin & Zuckerman 2008; Kilic, Gould & Koester 2009). Monitoring the stable pulsation arrival times of at least 6 white dwarfs can exclude >3 Jupiter-mass planets in a range of roughly 2 – 5 au (Winget et al. 2015). Unfortunately none of the most massive pulsating white dwarfs have stable, coherent modes that can be used to monitor for substellar companions.

dwarfs with atmospheric planetary remnants are suitable to low-resolution spectroscopic study in the near future with wide-area multi-object spectroscopic surveys such as WEAVE (Dalton et al. 2014), 4MOST (de Jong et al. 2019), DESI (DESI Collaboration et al. 2016) and SDSS-V (Kollmeier et al. 2017).

5.3 The smallest white dwarf hosts

The most massive known white dwarf planetary system hosts would also represent the smallest known white dwarf planetary system hosts. The classic mass-radius relation for white dwarfs (Nauenberg 1972)

$$\frac{R_{\star}}{R_{\odot}} \approx 0.0127 \left(\frac{M_{\star}}{M_{\odot}}\right)^{-1/3} \sqrt{1 - 0.607 \left(\frac{M_{\star}}{M_{\odot}}\right)^{4/3}} \quad (14)$$

yields, for the range of masses in Table 1, host star radii between $0.0013R_{\odot} - 0.0063R_{\odot} \approx 900 \text{ km} - 4,450 \text{ km} \approx 0.26R_{\text{Mars}} - 1.31R_{\text{Mars}}$. In contrast, a typical $0.6M_{\odot}$ white dwarf gives a radius of about $2.6R_{\text{Mars}}$.

How do the much smaller radii of the systems highlighted here affect the dynamical origin of metal pollution? The Roche radii of white dwarfs scale as $M_{\star}^{1/3}$ regardless of the composition or spin of orbiting companions (Veras et al. 2017). Therefore, doubling the white dwarf mass increases the Roche radii by about 25 per cent. This level of increase is significant, and can for example, trigger thermal self-disruption of passing gaseous planets which otherwise would be safe (Veras & Fuller 2019). The larger Roche radius also provides a larger target for minor planets, which, when combined with the location requirements for major planets in these systems, places restrictions on where and when scattering (Antoniadou & Veras 2016, 2019) occurs.

Another consequence of decreasing the size of a white dwarf and increasing its Roche radius is the resulting change in structure of a debris disc formed from the disruption of a minor planet (Graham et al. 1990; Jura 2003; Debes et al. 2012; Veras et al. 2014b, 2015b; Malamud & Perets 2020a,b). The outer edge would be larger than those of the currently known discs, increasing the probability of capture of solid objects (Grishin & Veras 2019); the consequences for the inner edge is less clear because of our lack of observations between the inner disc rim and the white dwarf photosphere. The resulting disc evolution and accretion rates onto the white dwarf might also differ from what has been previously modelled (Bochkarev & Rafikov 2011; Rafikov 2011a,b; Metzger et al. 2012; Rafikov & Garmilla 2012; Kenyon & Bromley 2017a,b; Miranda & Rafikov 2018).

5.4 Other features of 6M_⊙ – 8M_⊙ planetary systems

Major planets which form and reach distances of several to many au in under 70 Myr around $6M_{\odot} - 8M_{\odot}$ stars may help identify the dominant planet formation mechanisms in these systems. These planets formed in discs which are subject to time-varying radiative forcing at a more extreme level than their lower-host mass counterparts. When combined with photoevaporative effects from other stars in their birth cluster, outward migration of planets within these discs may

be enhanced (Veras & Armitage 2004; Rosotti et al. 2013, 2015; Ercolano & Rosotti 2015; Jennings et al. 2018).

If the $6M_{\odot} - 8M_{\odot}$ progenitor host stars for polluted white dwarfs were slightly more massive, then they would have instead become neutron stars; planets are known to exist around single pulsars (Wolszczan & Frail 1992; Wolszczan 1994; Konacki & Wolszczan 2003). These pulsar planets most likely represent products of second-generation planet formation from mergers or fallback (Currie & Hansen 2007; Margalit & Metzger 2017) although questions still remain (Hansen et al. 2009; Kerr et al. 2015)⁹. Exo-asteroids may orbit pulsars below the detection threshold (Cordes & Shannon 2008; Shannon et al. 2013; Dai et al. 2016; Smallwood et al. 2019b), although that threshold already lies at about 1 per cent of the mass of the Moon (Behrens et al. 2019).

In contrast, both major and minor planets orbiting single white dwarfs are first-generation, because the mass in the white dwarf debris discs required to form new planets is at the level of an Io mass or higher (van Lieshout et al. 2018). In contrast, the masses of white dwarfs with observed debris discs remain uncertain but are assumed (Vanderburg et al. 2015; Vanderbosch et al. 2019) to be generated instead by asteroids (with a typical mass two orders of magnitude less than Io). Further, the chemistry of any second-generation planets would be recycled from broken-up first generation bodies; Veras, Karakas & Gänsicke (submitted) demonstrate definitively that white dwarf pollution does not arise from stellar fallback.

6 SUMMARY

The most massive currently known progenitor of a white dwarf planetary system host ($\approx 4M_{\odot}$) exceeds the maximum mass of a main-sequence major planet host ($\approx 3M_{\odot}$). Because this mass difference is likely to increase with white dwarf population growth (Section 5.2), we have investigated major and minor planet survival limits for the highest possible stellar masses ($\approx 6M_{\odot} - 8M_{\odot}$) which yield white dwarfs. This mass regime represents almost completely unexplored territory for planet formation theorists, and largely unexplored territory for post-main-sequence planetary evolution investigators.

We found that a major planet needs to reside beyond 3-6 au (depending on the type of planet) at the end of the short (40-70 Myr) main-sequence phase in order to survive its host star transition into a white dwarf. Minor planets could have remained intact or broken up due to YORP-induced giant branch radiation, having been subject to host star luminosities reaching up to $10^5 L_{\odot}$. The boundary separating these two possibilities ($\sim 10^1 - 10^3$ au) is very sensitive to minor planet size, but is high enough to suggest that metal pollution in these systems would originate from already fragmented debris rather than intact minor planets

⁹ The sudden stellar mass loss experienced in a supernova is typically insufficient to eject a planet on a compact orbit (Veras et al. 2011). The more pertinent but outstanding question of first-generation planet survival is whether the planet can physically withstand a supernova's stellar ejecta.

which fragment upon reaching the white dwarf Roche radius. Our study motivates dedicated planet formation studies around the highest mass stars, and predicts that metal pollution can occur in the highest mass white dwarfs.

ACKNOWLEDGEMENTS

We thank the expert reviewer Fred C. Adams for helpful comments which have improved the manuscript. DV gratefully acknowledges the support of the STFC via an Ernest Rutherford Fellowship (grant ST/P003850/1). The research leading to these results has received funding from the European Research Council under the European Union's Horizon 2020 research and innovation programme no. 677706 (WD3D). Support for this work was also provided by NASA through grant number HST-GO-15073.005-A from the Space Telescope Science Institute, which is operated by AURA, Inc., under NASA contract NAS 5-26555. FM acknowledges support from the Royal Society Dorothy Hodgkin Fellowship. GMK is supported by the Royal Society as a Royal Society University Research Fellow. BTG is supported by the UK Science and Technology Facilities Council grant ST/P000495.

REFERENCES

- Adams, F. C., & Bloch, A. M. 2013, *ApJL*, 777, L30
 Adams, F. C., & Shu, F. H. 1986, *ApJ*, 308, 836
 Airapetian, V. S., & Usmanov, A. V. 2016, *ApJL*, 817, L24
 Antoniadou, K. I., & Veras, D. 2016, *MNRAS*, 463, 4108
 Antoniadou, K. I., & Veras, D. 2019, *A&A*, 629, A126
 Batygin, K., Bodenheimer, P. H., & Laughlin, G. P. 2016, *ApJ*, 829, 114
 Batygin, K., Adams, F. C., Brown, M. E., et al. 2019, *Physics Reports*, 805, 1
 Bauer, E. B., & Bildsten, L. 2018, *ApJL*, 859, L19
 Bauer, E. B., & Bildsten, L. 2019, *ApJ*, 872, 96
 Behrens, E. A., Ransom, S. M., Madison, D. R., et al. 2019, *arXiv:1912.00482*
 Bonsor, A., Mustill, A. J., & Wyatt, M. C. 2011, *MNRAS*, 414, 930
 Bochkarev, K. V., & Rafikov, R. R. 2011, *ApJ*, 741, 36
 Bonsor, A., Farihi, J., Wyatt, M. C., & van Lieshout, R. 2017, *MNRAS*, 468, 154
 Boss, A. P. 1997, *Science*, 276, 1836
 Brown, J. C., Veras, D., & Gänsicke, B. T. 2017, *MNRAS*, 468, 1575
 Cameron, A. G. W. 1978, *Moon and Planets*, 18, 5
 Campante, T. L., Veras, D., North, T. S. H., et al. 2017, *MNRAS*, 469, 1360
 Campbell, B., Walker, G. A. H., & Yang, S. 1988, *ApJ*, 331, 902
 Carlberg, J. K., Cunha, K., Smith, V. V., et al. 2012, *ApJ*, 757, 109
 Carlberg, J. K., Cunha, K., Smith, V. V., et al. 2013, *Astronomische Nachrichten*, 334, 120
 Cheng, S., Cummings, J. D., & Ménard, B. 2019, *arXiv e-prints*, *arXiv:1905.12710*
 Chiang, E. I., & Goldreich, P. 1997, *ApJ*, 490, 368
 Cordes, J. M., & Shannon, R. M. 2008, *ApJ*, 682, 1152
 Cotto-Figueroa, D., Statler, T. S., Richardson, D. C., et al. 2015, *ApJ*, 803, 25
 Coutu, S., Dufour, P., Bergeron, P., et al. 2019, *arXiv e-prints*, *arXiv:1907.05932*
 Covone, G., de Ritis, R., Dominik, M., et al. 2000, *A&A*, 357, 816
 Cummings, J. D., Kalirai, J. S., Tremblay, P.-E., et al. 2018, *ApJ*, 866, 21
 Cunningham, T., Tremblay, P.-E., Freytag, B., et al. 2019, *MNRAS*, 1723
 Currie, T., & Hansen, B. 2007, *ApJ*, 666, 1232
 Dai, Z. G., Wang, J. S., Wu, X. F., et al. 2016, *ApJ*, 829, 27
 Dalton, G., Trager, S., Abrams, D. C., et al. 2014, *Proceedings of the SPIE*, 91470L
 Debes, J. H., & Sigurdsson, S. 2002, *ApJ*, 572, 556
 Debes, J. H. 2006, *ApJ*, 652, 636
 Debes, J. H., Walsh, K. J., & Stark, C. 2012, *ApJ*, 747, 148
 Dennihy, E., Clemens, J. C., Dunlap, B. H., Fanale, S. M., Fuchs, J. T., Hermes, J. J. 2018, *ApJ*, 854, 40
 DESI Collaboration, Aghamousa, A., Aguilar, J., et al. 2016, *arXiv e-prints*, *arXiv:1611.00036*
 Dodson-Robinson, S. E., Veras, D., Ford, E. B., et al. 2009, *ApJ*, 707, 79
 Dosopoulou, F., & Kalogera, V. 2016a, *ApJ*, 825, 70
 Dosopoulou, F., & Kalogera, V. 2016b, *ApJ*, 825, 71
 Doyle, A. E., Young, E. D., Klein, B., et al. 2019, *Science*, 366, 356
 Dufour, P., Bergeron, P., Liebert, J., et al. 2007, *ApJ*, 663, 1291
 Dufour, P., Kilic, M., Fontaine, G., et al. 2010, *ApJ*, 719, 803
 Durisen, R. H., Boss, A. P., Mayer, L., et al. 2007, *Protostars and Planets V*, 607
 Ercolano, B., & Rosotti, G. 2015, *MNRAS*, 450, 3008
 Farihi, J., Becklin E. E., Zuckerman B., 2008, *ApJ*, 681, 1470
 Farihi, J., Dufour, P., Napiwotzki, R., et al. 2011, *MNRAS*, 413, 2559
 Farihi, J. 2016, *New Astronomy Reviews*, 71, 9
 Forgan, D. H., Ilee, J. D., Cyganowski, C. J., et al. 2016, *MNRAS*, 463, 957
 Frewen, S. F. N., & Hansen, B. M. S. 2014, *MNRAS*, 439, 2442
 Gallet, F., Bolmont, E., Mathis, S., Charbonnel, C., & Amard, L. 2017, *A&A*, 604, A112
 Gaia Collaboration, Brown, A. G. A., Vallenari, A., et al. 2018, *A&A*, 616, A1
 Gänsicke, B. T., Marsh, T. R., Southworth, J., & Rebassa-Mansergas, A. 2006, *Science*, 314, 1908
 Gänsicke, B. T., Koester, D., Farihi, J., et al. 2012, *MNRAS*, 424, 333
 Gänsicke, B., et al. 2019, *Published in Nature on 5 Dec, 2019*, doi:10.1038/s41586-019-1789-8
 García-Berro, E., Lorén-Aguilar, P., Aznar-Siguán, G., et al. 2012, *ApJ*, 749, 25
 Gentile Fusillo, N. P., Gänsicke, B. T., & Greiss, S. 2015, *MNRAS*, 448, 2260
 Gentile Fusillo, N. P., Tremblay, P.-E., Gänsicke, B. T., et al. 2019, *MNRAS*, 482, 4570
 Ghezzi, L., Montet, B. T., & Johnson, J. A. 2018, *ApJ*, 860, 109

- Girven, J., Brinkworth, C. S., Farihi, J., et al. 2012, *ApJ*, 749, 154
- Goldreich, P., & Ward, W. R. 1973, *ApJ*, 183, 1051
- Graham, J. R., Matthews, K., Neugebauer, G., & Soifer, B. T. 1990, *ApJ*, 357, 216
- Grishin, E., & Veras, D. 2019, *MNRAS*, 489, 168
- Grunblatt, S. K., Huber, D., Gaidos, E., et al. 2019, *AJ*, 158, 227
- Hadjidemetriou, J. D. 1963, *Icarus*, 2, 440
- Hansen, B. M. S., Shih, H.-Y., & Currie, T. 2009, *ApJ*, 691, 382
- Harris, A. W. 1978, in *Lunar and Planetary Inst. Technical Report, Vol. 9, Lunar and Planetary Institute Science Conference Abstracts*, 459461
- Harrison, J. H. D., Bonsor, A., & Madhusudhan, N. 2018, *MNRAS*, 479, 3814.
- Hatzes, A. P., & Cochran, W. D. 1993, *ApJ*, 413, 339
- Hayashi, C. 1981, *Progress of Theoretical Physics Supplement*, 70, 35
- Helled, R., Bodenheimer, P., Podolak, M., et al. 2014, *Protostars and Planets VI*, 643
- Hernández, J., Calvet, N., Hartmann, L., et al. 2005, *AJ*, 129, 856
- Hillwig, T. C., Jones, D., De Marco, O., et al. 2016, *ApJ*, 832, 125
- Hirabayashi, M., & Scheeres, D. J. 2019, *Icarus*, 317, 354
- Hollands, M. A., Koester, D., Alekseev, V., Herbert, E. L., & Gänsicke, B. T. 2017, *MNRAS*, 467, 4970
- Hollands, M. A., Gänsicke, B. T., & Koester, D. 2018, *MNRAS*, 477, 93.
- Hurley, J. R., Pols, O. R., & Tout, C. A. 2000, *MNRAS*, 315, 543
- Ilee, J. D., Cyganowski, C. J., Brogan, C. L., et al. 2018, *ApJL*, 869, L24
- Ingresso, G., Novati, S. C., de Paolis, F., et al. 2009, *MNRAS*, 399, 219
- Jankovic, M. R., Haworth, T. J., Ilee, J. D., et al. 2019, *MNRAS*, 482, 4673
- Jennings, J., Ercolano, B., & Rosotti, G. P. 2018, *MNRAS*, 477, 4131
- Jia, S., & Spruit, H. C. 2018, *ApJ*, 864, 169
- Johansen, A., Oishi, J. S., Mac Low, M.-M., et al. 2007, *Nature*, 448, 1022
- de Jong, R. S., Agertz, O., Berbel, A. A., et al. 2019, *The Messenger*, 175, 3
- Jura, M. 2003, *ApJL*, 584, L91
- Jura, M. 2008, *AJ*, 135, 1785
- Jura, M., & Young, E. D. 2014, *Annual Review of Earth and Planetary Sciences*, 42, 45
- Kepler, S. O., Pelisoli, I., Jordan, S., et al. 2013, *MNRAS*, 429, 2934
- Kepler, S. O., Pelisoli, I., Koester, D., et al. 2015, *MNRAS*, 446, 4078
- Kepler, S. O., Pelisoli, I., Koester, D., et al. 2016, *MNRAS*, 455, 3413
- Kennedy, G. M., & Kenyon, S. J. 2008, *ApJ*, 673, 502
- Kenyon, S. J., & Hartmann, L. 1987, *ApJ*, 323, 714
- Kilic M., Gould A., Koester D., 2009, *ApJ*, 705, 1219
- Kenyon, S. J., & Bromley, B. C. 2017a, *ApJ*, 844, 116
- Kenyon, S. J., & Bromley, B. C. 2017b, *ApJ*, 850, 50
- Kerr, M., Johnston, S., Hobbs, G., et al. 2015, *ApJL*, 809, L11
- Kervella, P., Homan, W., Richards, A. M. S., et al. 2016, *A&A*, 596, A92
- Kissin, Y., & Thompson, C. 2015, *ApJ*, 809, 108
- Kleinman, S. J., Kepler, S. O., Koester, D., et al. 2013, *ApJS*, 204, 5
- Koester, D. 2009, *A&A*, 498, 517
- Koester, D., Gänsicke, B. T., & Farihi, J. 2014, *A&A*, 566, A34
- Kollmeier, J. A., Zasowski, G., Rix, H.-W., et al. 2017, *arXiv e-prints*, arXiv:1711.03234
- Konacki, M., & Wolszczan, A. 2003, *ApJL*, 591, L147
- Kratter, K., & Lodato, G. 2016, *ARA&A*, 54, 271
- Kuiper, G. P. 1951, in *50th Anniversary of the Yerkes Observatory and Half a Century of Progress in Astrophysics*, ed. J. A. Hynek, 357
- Kunitomo, M., Ikoma, M., Sato, B., Katsuta, Y., & Ida, S. 2011, *ApJ*, 737, 66
- Lambrechts, M., & Johansen, A. 2012, *A&A*, 544, A32
- Laskar, J., & Gastineau, M. 2009, *Nature*, 459, 817
- Latham, D. W., Mazeh, T., Stefanik, R. P., et al. 1989, *Nature*, 339, 38
- Lissauer, J. J., & Stevenson, D. J. 2007, in *Protostars and Planets V*, ed. B. Reipurth, D. Jewitt, & K. Keil, 591606
- Lloyd, J. P. 2011, *ApJL*, 739, L49
- Lund, M. B., Pepper, J., & Stassun, K. G. 2015, *AJ*, 149, 16
- MacLeod, M., Cantiello, M., & Soares-Furtado, M. 2018, *ApJL*, 853, L1
- Madappatt, N., De Marco, O., & Villaver, E. 2016, *MNRAS*, 463, 1040
- Makarov, V. V., & Veras, D. 2019, *ApJ*, 886, 127
- Malamud, U., Perets, H. 2020a, Submitted to *MNRAS*
- Malamud, U., Perets, H. 2020b, Submitted to *MNRAS*
- Manser, C. J., et al. 2019, *Science*, 364, 66
- Marcy, G. W., & Butler, R. P. 1996, *ApJL*, 464, L147
- Margalit, B., & Metzger, B. D. 2017, *MNRAS*, 465, 2790
- Massarotti, A. 2008, *AJ*, 135, 2287
- Mayor, M., & Queloz, D. 1995, *Nature*, 378, 355
- Metzger, B. D., Rafikov, R. R., & Bochkarev, K. V. 2012, *MNRAS*, 423, 505
- Miranda, R., & Rafikov, R. R. 2018, *ApJ*, 857, 135
- Mizuno, H. 1980, *Progress of Theoretical Physics*, 64, 544
- Morbideilli, A., Nesvorny, D., Laurenz, V., et al. 2018, *Icarus*, 305, 262
- Mróz, P., & Poleski, R. 2018, *AJ*, 155, 154
- Mustill, A. J., & Villaver, E. 2012, *ApJ*, 761, 121
- Mustill, A. J., Veras, D., & Villaver, E. 2014, *MNRAS*, 437, 1404
- Mustill, A. J., Villaver, E., Veras, D., Gänsicke, B. T., Bonsor, A. 2018, *MNRAS*, 476, 3939.
- Nauenberg, M. 1972, *ApJ*, 175, 417
- Nelemans, G., & Tauris, T. M. 1998, *A&A*, 335, L85
- Nordhaus, J., & Blackman, E. G. 2006, *MNRAS*, 370, 2004
- Nordhaus, J., & Spiegel, D. S. 2013, *MNRAS*, 432, 500
- North, T. S. H., Campante, T. L., Miglio, A., et al. 2017, *MNRAS*, 472, 1866
- Omarov, T. B. 1962, *Izv. Astrofiz. Inst. Acad. Nauk. KazSSR*, 14, 66
- Payne, M. J., Veras, D., Holman, M. J., Gänsicke, B. T. 2016, *MNRAS*, 457, 217
- Payne, M. J., Veras, D., Gänsicke, B. T., & Holman, M. J. 2017, *MNRAS*, 464, 2557

- Perri, F., & Cameron, A. G. W. 1974, *Icarus*, 22, 416
- Perryman, M., Hartman, J., Bakos, G. Á., et al. 2014, *ApJ*, 797, 14
- Polishook, D., Moskovitz, N., Thirouin, A., et al. 2017, *Icarus*, 297, 126
- Pollack, J. B. 1984, *ARA&A*, 22, 389
- Pyrzas, S., Gänsicke, B. T., Brady, S., et al. 2012, *MNRAS*, 419, 817
- Rafikov, R. R. 2011a, *MNRAS*, 416, L55
- Rafikov, R. R. 2011b, *ApJL*, 732, L3
- Rafikov, R. R., & Garmilla, J. A. 2012, *ApJ*, 760, 123
- Rao S., et al., 2018, *A&A*, 618, A18
- Reffert, S., Bergmann, C., Quirrenbach, A., et al. 2015, *A&A*, 574, A116
- Rice, K. 2016, *PASA*, 33, e012
- Rosotti, G. P., Ercolano, B., Owen, J. E., et al. 2013, *MNRAS*, 430, 1392
- Rosotti, G. P., Ercolano, B., & Owen, J. E. 2015, *MNRAS*, 454, 2173
- Rozitis, B., & Green, S. F. 2012, *MNRAS*, 423, 367
- Rozitis, B., & Green, S. F. 2013, *MNRAS*, 430, 1376
- Safronov, V. S., & Zvjagina, E. V. 1969, *Icarus*, 10, 109
- Sánchez, P., & Scheeres, D. J. 2014, *Meteoritics and Planetary Science*, 49, 788
- Sanna, A., Kölligan, A., Moscadelli, L., et al. 2019, *A&A*, 623, A77
- Sato, B., Omiya, M., Harakawa, H., et al. 2012, *PASJ*, 64, 135
- Schatzman, E. 1945, *Annales d'Astrophysique*, 8, 143
- Schatzman, E. 1947, *Annales d'Astrophysique*, 10, 19
- Scheeres, D. J. 2007, *Icarus*, 188, 430
- Scheeres, D. J., Britt, D., Carry, B., et al. 2015, *Asteroids IV*, 745
- Scheeres, D. J. 2018, *Icarus*, 304, 183
- Shannon, R. M., Cordes, J. M., Metcalfe, T. S., et al. 2013, *ApJ*, 766, 5
- Shen, K. J., Bildsten, L., Kasen, D., et al. 2012, *ApJ*, 748, 35
- Smallwood, J. L., Martin, R. G., Livio, M., & Lubow, S. H. 2018, *MNRAS*, 480, 57
- Smallwood, J. L., Martin, R. G., Livio, M. 2019a, Submitted to *MNRAS*
- Smallwood, J. L., Martin, R. G., & Zhang, B. 2019b, *MNRAS*, 485, 1367
- Smartt, S. J. 2009, *ARA&A*, 47, 63
- Staff, J. E., De Marco, O., Wood, P., Galaviz, P., & Passy, J.-C. 2016, *MNRAS*, 458, 832
- Stello, D., Huber, D., Grundahl, F., et al. 2017, *MNRAS*, 472, 4110
- Stephan, A. P., Naoz, S., Gaudi, B. S., et al. 2019, Submitted to *ApJ*, arXiv:1909.05259
- Sun, M., Arras, P., Weinberg, N. N., et al. 2018, *MNRAS*, 481, 4077
- Swan, A., Farihi, J., Koester, D., et al. 2019, *MNRAS*, 490, 202
- Temmink, K. D., Toonen, S., Zapartas, E., et al. 2019, arXiv e-prints, arXiv:1910.05335
- Toonen, S., Nelemans, G., & Portegies Zwart, S. 2012, *A&A*, 546, A70
- Toonen S., Hollands M., Gänsicke B. T., Boekholt T., 2017, *A&A*, 602, A16
- Tremblay, P.-E., Bergeron, P., & Gianninas, A. 2011, *ApJ*, 730, 128
- Tremblay P.-E., Cummings J., Kalirai J. S., Gänsicke B. T., Gentile-Fusillo N., Raddi R., 2016, *MNRAS*, 461, 2100
- Tsiganis, K., Gomes, R., Morbidelli, A., et al. 2005, *Nature*, 435, 459
- van Maanen, A. 1917, *PASP*, 29, 258
- van Maanen, A. 1919, *AJ*, 32, 86
- van Lieshout, R., Kral, Q., Charnoz, S., et al. 2018, *MNRAS*, 480, 2784.
- Vanderbosch, Z., Hermes, J. J., Denny, E., et al. 2019, Submitted to *ApJL*, arXiv:1908.09839
- Vanderburg, A., Johnson, J. A., Rappaport, S., et al. 2015, *Nature*, 526, 546
- Veras, D., & Armitage, P. J. 2004, *MNRAS*, 347, 613
- Veras, D., Wyatt, M. C., Mustill, A. J., et al. 2011, *MNRAS*, 417, 2104
- Veras, D., & Wyatt, M. C. 2012, *MNRAS*, 421, 2969
- Veras, D., Mustill, A. J., Bonsor, A., & Wyatt, M. C. 2013a, *MNRAS*, 431, 1686
- Veras, D., Hadjidemetriou, J. D., & Tout, C. A. 2013b, *MNRAS*, 435, 2416
- Veras, D., Leinhardt, Z. M., Bonsor, A., Gänsicke, B. T. 2014b, *MNRAS*, 445, 2244
- Veras, D., Jacobson, S. A., Gänsicke, B. T. 2014a, *MNRAS*, 445, 2794
- Veras, D., Gänsicke, B. T. 2015, *MNRAS*, 447, 1049
- Veras, D., Eggl, S., Gänsicke, B. T. 2015a, *MNRAS*, 451, 2814
- Veras, D., Leinhardt, Z. M., Eggl, S., et al. 2015b, *MNRAS*, 451, 3453
- Veras, D. 2016a, *Royal Society Open Science*, 3, 150571
- Veras, D. 2016b, *MNRAS*, 463, 2958
- Veras, D., Mustill, A. J., Gänsicke, B. T., et al. 2016, *MNRAS*, 458, 3942
- Veras, D., Carter, P. J., Leinhardt, Z. M., & Gänsicke, B. T. 2017, *MNRAS*, 465, 1008
- Veras, D., Xu, S., & Rebassa-Mansergas, A. 2018a, *MNRAS*, 473, 2871
- Veras D., Georgakarakos N., Gänsicke B. T., Dobbs-Dixon I., 2018b, *MNRAS*, 481, 2180
- Veras, D., Higuchi, A., Ida, S. 2019b, *MNRAS*, 485, 708
- Veras, D., Efroimsky, M., Makarov, V. V., et al. 2019a, *MNRAS*, 486, 3831
- Veras, D., & Fuller, J. 2019, *MNRAS*, 489, 2941
- Veras, D., & Fuller, J. 2020, Submitted to *MNRAS*, arXiv:1912.02199
- Veras, D., & Scheeres, D. 2020, In Press *MNRAS*, arXiv:2001.00949
- Veras, D., & Wolszczan, A. 2019, *MNRAS*, 488, 153
- Villaver, E., & Livio, M. 2009, *ApJL*, 705, L81
- Villaver, E., Livio, M., Mustill, A. J., & Siess, L. 2014, *ApJ*, 794, 3
- Vokrouhlický, D., Bottke, W. F., Chesley, S. R., et al. 2015, *Asteroids IV*, 509
- Voyatzis, G., Hadjidemetriou, J. D., Veras, D., & Varvoglis, H. 2013, *MNRAS*, 430, 3383
- Wada, K., Tsukamoto, Y., & Kokubo, E. 2019, submitted to *ApJ*, arXiv:1909.06748
- Warner, B. D., Harris, A. W., Pravec, P. 2009, *Icarus*, 202, 134
- Wilson, T. G., Farihi, J., Gänsicke, B. T., et al. 2019, *MNRAS*, 487, 133

- Winget D. E., et al., 2015, ASPC, 285, ASPC..493
Wolszczan, A., & Frail, D. A. 1992, Nature, 355, 145
Wolszczan, A. 1994, Science, 264, 538
Youdin, A. N., & Goodman, J. 2005, ApJ, 620, 459
Yu, Y., Michel, P., Hirabayashi, M., et al. 2018, AJ, 156, 59
Zahn, J.-P. 1977, A&A, 500, 121
Zuckerman, B., & Becklin, E. E. 1987, Nature, 330, 138